analytical chemistry

Article

pubs.acs.org/ac

One-Dimensional Approach to Study Kinetics of Reversible Binding of Protein on Capillary Walls

Leonid T. Cherney, Alexander P. Petrov, and Sergey N. Krylov*

[†]Department of Chemistry and Centre for Research on Biomolecular Interactions, York University, Toronto, Ontario M3J 1P3, Canada

ABSTRACT: We introduce a method for kinetic characterization of reversible binding of protein onto the inner capillary wall. In essence, a short plug of the protein solution is propagated through the capillary by pressure, and the protein is detected at the distal capillary end. The signal versus time profile is fitted with a numerical model which uses the rate constants of adsorption, k_{ad}, and desorption, k_{de}, as fitting parameters. The values of k_{ad} and k_{de} which result in the best fit are considered to be the sought ones. We first used COMSOL multiphysics software to develop a numerical model with two-dimensional (2D) equations of mass transfer. Although 2D models in general can describe experiments more accurately than one-dimensional (1D) models, computing 2D models takes much more time (many hours to find two parameters: k_{ad} and k_{de}). We used the fact that the capillary is narrow and long to develop a simplified model with 1D equations of mass transfer. Our comparison of the 1D and 2D models showed that the errors of the 1D approximation were less than 5%, whereas the computation of the 1D model was 100 times faster. We finally used the 1D approach to study kinetics of reversible binding of conalbumin to the uncoated fused-silica capillary walls. We determined k_{ad}, k_{de}, and a diffusion coefficient, D. The obtained value of D is in excellent agreement with literature data which suggests that the values of k_{ad} and k_{de} (for which there are no literature data) are also calculated correctly. Our approach for finding k_{ad} and k_{de} will facilitate quantitative characterization of protein adsorption on capillary walls as well as properties of passivating materials used for capillary coating.

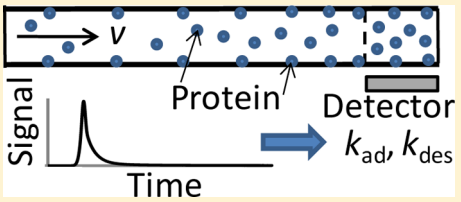

Protein adsorption onto the inner capillary walls can significantly affect various protein analyses by capillary electrophoresis (CE).[1−4] In particular, it can obscure studies of biomolecular interactions and aptamer selection by methods of kinetic capillary electrophoresis (KCE).[4] Protein adsorption to fused-silica capillaries can be caused by silanol groups on the inner surface which are negatively charged at physiological pH.[5,6] A straightforward approach to reducing the protein−surface interactions would be to decrease pH to values at which the surface charge decreases or to increase pH to values higher than the isoelectric point of protein making protein molecules also negatively charged.[7,8] However, this approach cannot be applied when maintaining the native structure of the protein is essential. A more versatile way of preventing protein adsorption employs temporary or permanent coatings that mask the fused silica surface.[9,10] To justifiably choose a material for the coating, one needs information on quantitative characteristics of reversible binding. The most important characteristics are kinetic rate constants of adsorption and desorption, k_{ad} and k_{de}. Knowledge of these two rate constants can help to characterize the properties of different coatings and to account for the adsorption and desorption processes in CE when they cannot be avoided or, on the contrary, are employed for some purpose.

Protein adsorption to surfaces plays an important role in living organisms and in many technologies.[11,12] Various methods have been used in studying this phenomenon.[13−26] Among them are ellipsometry,[14,15] reflectometry,[16−19] temperature-jump relaxation technique,[20] surface plasmon resonance,[21] optical waveguide spectroscopy,[22] total internal reflection (TIR) fluorescence with photobleaching recovery,[23] TIR fluorescence correlation spectroscopy,[23,24] TIR fluorescence microscopy,[25] and TIR Raman spectroscopy.[26] To the best of our knowledge, all studies have been carried out in flow cells with dimensions significantly larger than the inner diameter of capillaries used in CE. The flow-cell geometry is usually quite different as well. Adsorption and desorption processes drastically depend on the surface properties and on compounds the surface has been in contact with previously. Given these facts, standard methods are practically inapplicable to studying adsorption and desorption characteristics of the inner surface of narrow capillaries usually used in CE. The best way for studying protein adsorption to the material of such capillaries would be to perform adsorption studies in these capillaries. Because protein adsorption can significantly affect electroosmotic flow (EOF), it is preferable to use pressure (rather than EOF) for injection and propagation of the protein solution plug.[4] The deformation of the protein plug shape (due to adsorption and desorption processes) during its movement through the capillary can be used to find k_{ad}, k_{de}, and other relevant parameters. Such an approach has multiple advantages. First, it allows one to work with extremely small amounts of the protein. Second, it directly demonstrates the effect of adsorption and desorption on propagation patterns of the protein. Third, studies in capillaries allow one to investigate the

Received: October 16, 2014
Accepted: December 14, 2014
Published: December 14, 2014

DOI: 10.1021/ac503880j
Anal. Chem. 2015, 87, 1219−1225

actual inner surface of capillaries rather than samples that mimic them. Fourth, simplified one-dimensional (1D) models can be used for data processing, whereas rigorous studies in usual flow cells require solving at least two-dimensional (2D) problems. Fifth, studies in very narrow capillaries are usually surface-reaction limiting, which allows one to analyze adsorption and desorption effects in pure form eliminating the influence of transverse diffusion to the capillary walls.

Pressure-driven propagation of a protein plug through the capillary is experimentally simple. The challenge is to find a mathematical model that can adequately describe the adsorption/desorption processes and facilitate finding the binding parameters. In a pattern-based approach, a mathematical solution should be fitted into the signal-vs-time profile generated by the protein passing the detector at the end of the capillary. Such fitting is performed at various values of k_{ad}, k_{de}, and other relevant parameters until the best fit is found. The values of parameters that result in the best fit are, by definition, the best approximation of real values of these parameters. In an alternative parameter-based approach, a mathematical solution would be used to obtain approximate expressions for k_{ad}, k_{de}, other parameters in terms of some easily measured characteristics (e.g., peak areas and migration times) of the signal-vs-time profile from the eluting protein.

Here, we extended the axially dispersed plug flow model[27] by adding reactions at the capillary wall. As a result, we use 1D equations for the average (across the capillary) volume concentration of protein that was present in the initial plug and for the surface concentration of the adsorbed protein. These equations take into account the average velocity of the liquid flow, effective longitudinal diffusion, and the processes of adsorption and desorption on the capillary wall as well as the spatial (along the capillary) and temporal dependences of protein concentrations. We include effective longitudinal diffusion because it may affect the concentration profile in the protein plug. Transverse diffusion does not appear in the equations since they are averaged across the capillary (i.e., they are formulated for the average protein concentration in the capillary cross-section). Such a 1D approach is only applicable to capillaries which are sufficiently narrow and long to satisfy the requirement that the characteristic diffusion time across the capillary is smaller than characteristic times of adsorption, desorption, and plug passage through the capillary. Mechanisms of protein adsorption can be very complex and include both reversible and irreversible binding.[14,15,18,19,21−23] Special techniques were developed to study irreversible adsorption.[28−31] Irreversible adsorption can be negligible in a capillary if the adsorbed protein is quickly exposed to protein-free solution (if the protein plug is short). The main purpose of this work was to develop a simple and effective method of quantitative analysis of protein adsorption−desorption in CE rather than to analyze different adsorption models. Thus, the simplest model of reversible protein adsorption is considered below. For such a model, we obtained numerical solutions of 1D equations and verified them using numerical solutions of the full 2D problem. The 1D approach was then tested by fitting signals-vs-time profiles simulated with 1D equations into experimental signal-vs-time profiles. We also studied the influence of binding parameters on signal-vs-time profiles.

RESULTS AND DISCUSSION

Basic Equations of Mass Transfer in the Presence of Adsorption and Desorption. We consider the following setup (Figure 1). A long and narrow capillary is coaxial with the x coordinate. A short plug of length W containing a protein, A,

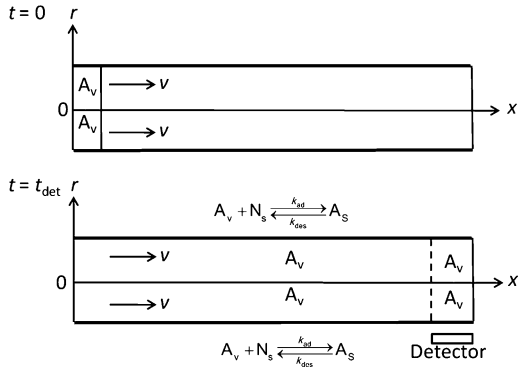

Figure 1. Schematic of a setup for studying reversible binding of protein to a capillary in a flow. The top panel shows the initial plug containing protein molecules A_v right after injecting it into the capillary at $t = 0$. The bottom panel shows the plug when it reaches the detector at $t = t_{det}$ (the plug rear boundary is shown by a dashed line). Protein molecules A_s adsorbed on the wall and protein molecules A_v in free volume are left in the trail behind the plug. Molecules A_v in the trail result from partial desorption of protein from the wall. The detector measures a signal that gradually decreases with time $t > t_{det}$.

is injected at time $t = 0$. The buffer outside the plug does not contain the protein. A flow in the capillary is caused by pressure difference at the capillary ends, the velocity profile is parabolic with no radial velocity present.

A reversible binary reaction of adsorption−desorption (1) takes place on the capillary walls:

$$A_v + N_s \underset{k_{de}}{\overset{k_{ad}}{\rightleftarrows}} A_s, \qquad K_{ad} \equiv \frac{k_{ad}}{k_{de}} \tag{1}$$

were, A_v, N_s, and A_s denote free protein in the volume, free adsorption sites on the surface, and protein bound to the surface, respectively. We neglect possible conformational changes in protein upon its adsorption to the surface and consider only the reversible adsorption reaction 1. Desorption of the protein adsorbed onto the walls can be started when the protein plug moves further and the adsorbed protein contacts with the protein-free buffer, which arrives in <10 s after adsorption (for plug length $W < 1$ cm and plug velocity $v > 0.1$ cm/s). Conformational changes in the adsorbed protein typically require much longer times.[14,15,18] By definition, the adsorption and desorption rates, q_{ad} and q_{de}, are related to k_{ad} and k_{de} as follows:

$$q_{ad} = k_{ad}A_vN_s,\ q_{de} = k_{de}A_s,\ N_s = N_{tot} - A_s \tag{2}$$

where A_v is the volume concentration of A_v; N_s and A_s are the surface concentrations of N_s and A_s; N_{tot} is the total concentration of occupied and free binding sites on the surface. Parameters q_{ad} and q_{de} have units of mol/(cm^{2}s). N_{tot} can be also defined as the maximum possible value of A_s. In the equilibrium, $q_{ad} = q_{de}$ and eqs 1 and 2 result in the following relation:

$$\frac{A_s^{eq}}{A_v^{eq}(N_{tot} - A_s^{eq})} = K_{ad} \tag{3}$$

DOI: 10.1021/ac503880j
Anal. Chem. 2015, 87, 1219−1225

where the superscript refers to the state of equilibrium. Mass transfer of A_v and A_s in the presence of adsorption and desorption is described by equations:[32,33]

$$\left(\partial_t + 2v\left(1 - \frac{r^2}{R^2}\right)\partial_x\right)A_v = D\left(\partial_x^2 + \frac{1}{r}\partial_r r\partial_r\right)A_v \quad (4)$$

$$\partial_t A_s = D_s\partial_x^2 A_s + q_{ad} - q_{de},\ D(\partial_r A_v)_{r=R} = q_{de} - q_{ad} \quad (5)$$

where, v is the velocity averaged across the capillary; r is the distance from the capillary axis; R is the inner radius of the capillary; ∂_x, ∂_r, and ∂_t are partial derivations by the spatial coordinates x and r and by time t, respectively; D is the diffusion coefficient of A_v; D_s is the surface diffusion coefficient of A_s (it describes diffusion of A_s over adsorption sites). Equation 4 is valid in the capillary volume, whereas the relationships of eq 5 should work on the inner surface of the capillary.

Equation 4 and the first eq 5 express in the differential form the mass conservation laws for the protein dissolved in the volume and the protein bound at the surface, respectively.[32,33] The last eq 5 expresses the mass conservation law for reactions of adsorption and desorption between the protein dissolved in the volume and the protein bound at the surface. Equations 4 and 5 can be also derived from the corresponding integral conservation laws for protein.[32] We used a parabolic velocity profile in eq 4 following the Taylor's approach to studying flows of dispersions in long capillaries with $R/L \ll 1$.[34−36]

Boundary conditions for a plug injected at the capillary inlet and for a free flow at the capillary outlet can be formulated as follows:

$$A_v(t) = A_0,\ (0 \le t \le t_0 = W/v)$$
$$A_v(t) = 0,\ (t > t^0) \quad \text{at } x = 0 \quad (6)$$

$$D\partial_x A_v = 0,\ (t \ge 0) \quad \text{at } x = L \quad (7)$$

$$D_s\partial_x A_s = 0,\ (t \ge 0) \quad \text{at } x = 0, L \quad (8)$$

Here, the origin of the x axis coincides with the capillary inlet, and L is the capillary length. Finally, initial conditions for A_v and A_s express the absence of the protein in the initial buffer that fills the capillary at $t = 0$:

$$A_v(x) = 0, \quad A_s(x) = 0 \quad \text{at } t = 0 \quad (9)$$

One-Dimensional Approximation. In general, the 2D time-dependent system of eqs 2, 4, and 5 with boundary and initial conditions 6−9 can be solved only numerically. Unfortunately, numerical solutions require significant computational times for narrow capillaries. In some cases, finding a solution can take many hours of computing even for only two variable parameters, k_{ad} and k_{de}. The long calculation is caused by a small value of R/L (typically $<10^{-4}$). On the other hand, the small value of R/L suggests that averaging (across the capillary) can be used to transform the 2D problem into a 1D problem. Strictly speaking, this transformation is possible if the characteristic time of transverse diffusion, $t_{trans} = R^2/D$, is much smaller than the characteristic adsorption and desorption times and the characteristic flow time to the detector, $t_{det} = L/v$. Such condition is usually satisfied for very narrow and long capillaries ($R \le 40$ μm, $L \ge 10$ cm) in sufficiently large ranges of k_{ad}, k_{de}, and N_{tot}. In this case, one can assume that a relative variation of protein concentration across the capillary is small. This fact allows the Taylor's approach to describing dispersions[34−37] to be used in the averaging procedure. As a result, the following 1D equations can be derived from 2D eqs 2, 4, and 5:

$$(\partial_t + v\partial_x)A = D_T\partial_x^2 A - \frac{2}{R}(k_{ad}A(N_{tot} - A_s) - k_{de}A_s) \quad (10)$$

$$\partial_t A_s = D_s\partial_x^2 A_s + k_{ad}A(N_{tot} - A_s) - k_{de}A_s \quad (11)$$

where, A is the average (across the capillary) value of A_v, D_T is the effective longitudinal diffusion coefficient determined by Taylor's expression:[34−36]

$$D_T = D\left(1 + \frac{\mathrm{Pe}^2}{48}\right),\ \mathrm{Pe} = \frac{vR}{D} \quad (12)$$

where Pe is the Peclet number. The Taylor correction depends on the Peclet number, Pe, and is significant because, in our case, Pe = 625 (at $v = 0.1$ cm/s, $R = 37.5$ μm, and $D = 6 \times 10^{-7}$ cm^2s^{-1}). Actually, the unity in expression (12) for the effective diffusion coefficient can be neglected in comparison to the Taylor correction.

The main assumption used in the r-averaging procedure is that the variation of protein concentration is much smaller than the average protein concentration (for given x). This assumption is satisfied if condition $L \gg \mathrm{Pe}R$ is hold.[34−36] The strong inequality guarantees that for time L/v required to travel through the capillary the characteristic diffusion length of the protein $(DL/v)^{1/2}$ is much larger than the capillary radius. Thus, diffusion can almost smooth the differences in the concentration across the capillary. In our case, we have Pe = 625 and the required condition is approximately held for 10 and 40 cm-long capillaries. The averaging procedure in the absence of adsorption and desorption results in eq 10 without terms depending on k_{ad} and k_{de}.[34−36] The averaging procedure in the presence of adsorption and desorption was described in the Supporting Information to our earlier work.[37] In that work, it was shown that the combination of binding dynamics at the boundaries is consistent with Taylor's dispersion. Processes of adsorption and desorption lead to the addition of terms depending on k_{ad} and k_{de} in eq 10. These terms describe the decrease and increase of protein concentration in the volume caused by adsorption and desorption, respectively. Equation 11 was obtained by a substitution of expressions (2) into the first eq 5.

Further simplification of the boundary conditions (at the capillary inlet and outlet) and initial conditions for eqs 10 and 11 can be easily obtained from equations 6−9 by replacing A_v with A. According to eqs 10 and 11, characteristic times of adsorption, t_{ad}, and desorption, t_{de}, can be defined as follows:

$$t_{ad} = \frac{R}{2k_{ad}N_{tot}}, \quad t_{de} = \frac{1}{k_{de}} \quad (13)$$

Numerical solution of eqs 10 and 11 are much simpler than that of eqs 4 and 5 since the system of eqs 10 and 11 is formulated in the 1D domain ($0 \le x \le L$), whereas the system of eqs 4 and 5 must to be solved in the 2D domain ($0 \le x \le L$, $0 \le r \le R$).

Comparison of 1D and 2D Models and Fitting Experimental Data. Solution of the 2D problem (eqs 4−9) (or the 1D problem (eqs 10−12) with corresponding initial and boundary conditions) results in dependencies of protein (volume and surface) concentrations on spatial coordinates and

DOI: 10.1021/ac503880j
Anal. Chem. 2015, 87, 1219−1225

time. On the other hand, experimental data operate with signals measured at the specific coordinate $x = x_{det}$ where the detector is placed (see Figure 1). The protein signal, S, is usually proportional to the linear concentration (i.e., to the amount per unit length of the capillary) of the protein at this coordinate:

$$S(t) = g\pi R^2 A(t) + g_s 2\pi R A_s(t), \quad g = \frac{Q}{\chi}, \quad g_s = \frac{Q_s}{\chi_s} \tag{14}$$

Coefficients g and g_s are determined by the nature of a signal used to detect the protein. For example, in the case of fluorescence detection, g and g_s are determined by the second and third relations (eq 14), where Q and Q_s are the absolute quantum yields. Coefficients χ and χ_s depend on the nature of fluorophore and the parameters of the detector.[38,39]

To verify accuracy of our 1D approach we compared it with the 2D approach. Calculations were performed with COMSOL Multiphysics 4.2 commercial software (COMSOL Group, Palo Alto, CA). First, simulated signals were obtained using eqs 10, 11, and 14 (1D model) at various sets of parameters k_{ad}, k_{de}, N_{tot}, D, v, R, L, A_0, t_0, g, x_{det}. The surface diffusion was neglected since $D_s \ll D_T$ for all values of D, v, and R used in simulations. A mesh with 300 elements was used for FEM calculations in COMSOL. The distribution was normal and the finite element method was used for simulations. Equations 10 and 11 were integrated using the Transport of Diluted Species module in COMSOL. Then we performed similar calculations based on eqs 4, 5, and 14 (2D approach) for the same sets of parameters. Comparison of results at three different signal patterns is presented in Figure 2 (signals for 1D and 2D models are shown by solid red lines and dashed black lines, respectively). The difference between 1D and 2D simulations in Figure 2 can be quantified by calculating Normalized Root Mean Square Deviation (NRMSD),[40] and NRMSD can be considered as a relative error. It was 0.7%, 4.3%, and 4.7% for panels A, B, and C, respectively, in Figure 2. Such agreement is sufficient for quantitatively studying protein adsorption and desorption in CE. The 1D approach is sufficiently accurate and leads to a reduction in computing time from tens of hours to several minutes. We also used the simulated 2D data of Figure 2 as input data for the 1D model and performed a fit of parameters k_{ad}, k_{de}, D, and N_{tot}. Simulated signals for such a fit are shown by solid green lines in Figure 2. As a result we found that the best fit of the 1D model into the 2D model corresponds to values of k_{ad}, k_{de}, D, and N_{tot} that differ, respectively, by 2%, 2%, 1%, and 6% from values of k_{ad}, k_{de}, D, and N_{tot} used in 2D simulations shown in panel A of Figure 2. For 2D simulations presented in panels B and C of Figure 2, these errors for k_{ad}, k_{de}, D, N_{tot} were 10%, 4%, 1%, 10% and 9%, 3%, 7%, 3%, respectively. Such errors are acceptable for the practical use in CE. It should be noted that signals for the best fits of 1D model into 2D simulated data practically coincide with the 1D direct simulations (shown by red lines in Figure 2) in almost the entire time range. We used the Levenberg–Marquardt method for fitting in COMSOL. The objective function was the least-squares differences between the points of experimental (or simulated) data and theoretical model.

To test the 1D approach in the determination of k_{ad} and k_{de}, we used data from experimental studies of conalbumin (from hen egg white) propagation through the capillary described elsewhere.[4] These data were obtained for the pressure driven propagation of a solution plug containing conalbumin at two

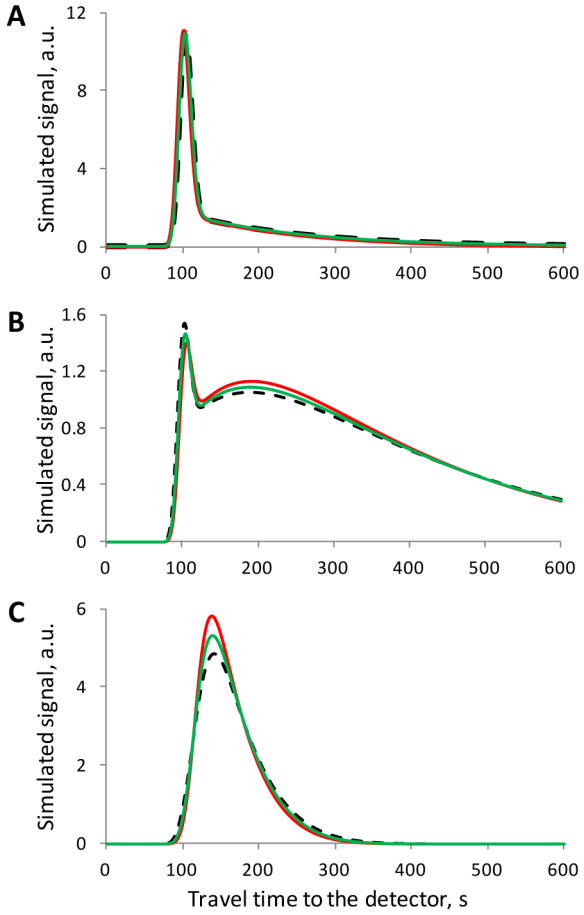

Figure 2. Comparison of signal simulations based on 1D (solid red lines) and 2D (dashed black lines) models. Various sets of adsorption and desorption rate constants were probed: (**A**) k_{ad} = 10 $(mM)^{-1}$ s^{-1}, k_{de} = 0.01 s^{-1}; (**B**) k_{ad} = 45 $(mM)^{-1}s^{-1}$, k_{de} = 0.012 s^{-1}; (C) k_{ad} = 100 $(mM)^{-1}s^{-1}$, k_{de} = 0.1 s^{-1}. Other parameters were the same in all three panels. The best fits of 1D model into the 2D simulated data are shown by solid green lines.

different initial concentrations. Conalbumin is a moderately adsorptive protein, and it was used to qualitatively analyze protein adsorption in CE.[4] It was fluorescently labeled for detection. The plug of 5.3 μM conalbumin was injected during 5 s, whereas the plug of 6.2 μM conalbumin was injected during 6 s. Distances of 10 and 40 cm from the injection end to the detector were used for each conalbumin concentration. Experiments were repeated five times. Numerical solutions of eqs 10 and 11 were found with COMSOL Multiphysics 4.2 software. These solutions and expression (eq 14) were used to calculate signals corresponding to the 1D model (for simplicity, we assume that $g_s = g$ in eq 14). These signals were then fitted into experimental data by varying parameters k_{ad}, k_{de}, D, and N_{tot} until the best fit was found. The coefficient g was also determined from the best fit but only in three experiments to confirm a stable solution for it. Then, the obtained average value of g was used in the best fit procedure applied to all other experiments. Calculations showed that the best fit presented in Figures 3 and 4 can be achieved when the surface concentration of protein is far from saturation (i.e., $A_s \ll N_{tot}$). In this case, the best fit can determine only the product $k_{ad}N_{tot}$, which is essential in eqs 10 and 11 at $A_s \ll N_{tot}$. The product $k_{ad}N_{tot}$ is used to calculate t_{ad} with expressions (eq 13). The value of N_{tot} can be estimated as follows. The crystallographic structure of

DOI: 10.1021/ac503880j
Anal. Chem. 2015, 87, 1219–1225

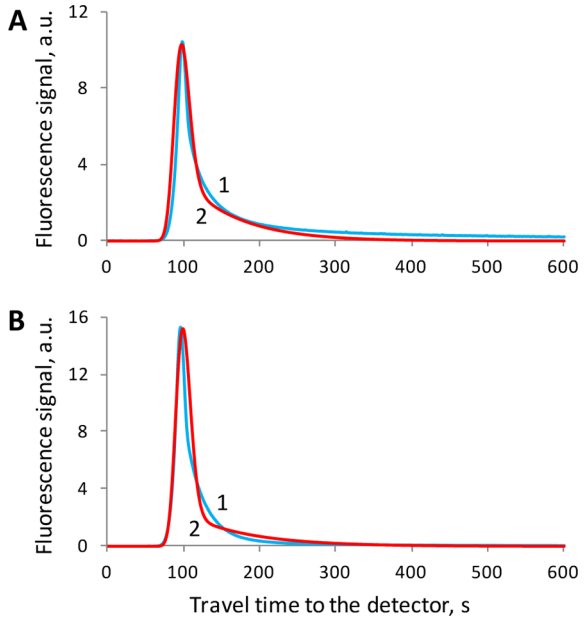

Figure 3. Distance to the detector is 10 cm. The best fit of the signal generated with the 1D model (red lines 2) into experimental data for conalbumin (blue lines 1) for the initial concentration of protein in the plug being A_0 = 5.3 μM (**A**) and 6.2 μM (**B**).

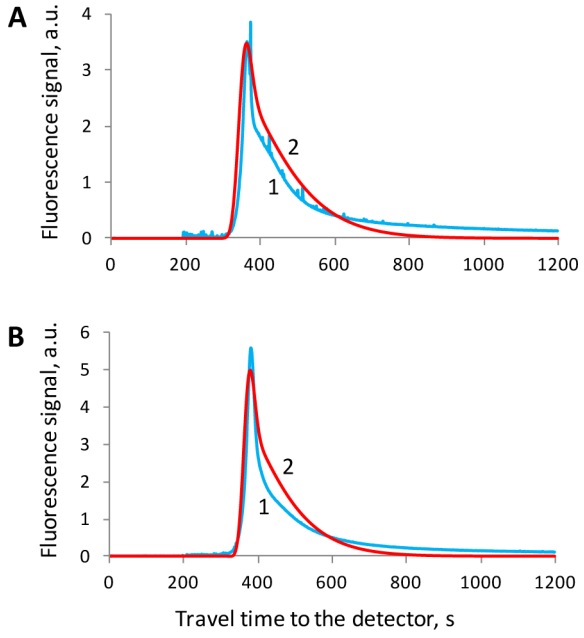

Figure 4. Distance to detector is 40 cm. The best fit of the signal generated with the 1D model (red lines 2) into experimental data for conalbumin (blue lines 1) for the initial concentration of protein in the plug being A_0 = 5.3 μM (**A**) and 6.2 μM (**B**).

conalbumin molecule[41] (PDB code 1AIV) gives a value of ~100 Å for its maximum diameter d. Thus, one adsorbed molecule occupies ~10^4 Å^2 of the wall surface. Given the average surface area of 20 Å^2 per silanol group on the silica surface[5,6] and pK_a values of 4.9 and 8.5 for isolated and vicinal silanol groups (with corresponding surface populations of 19 and 81%, respectively),[6,42] we can assume that a conalbumin molecule can be adsorbed at any location at the fused silica surface of capillary. Therefore, $N_{tot} \sim 1/(d^2 N_A) \sim 2 \times 10^{-12}$ mol/cm^2 where N_A is the Avogadro number. Inequality $A_s \ll N_{tot}$ is valid for practically all initial protein concentrations and for all plug/capillary dimensions practically used in CE ($A_0 \leq 1$ μM, $W \leq 1$ cm, $R \leq 100$ μm, and $L \geq 10$ cm) even if all protein molecules are adsorbed from the plug.

The fit to experimental results for times much longer than the travel time of the plug is worse than the fit to the peak itself. One possible explanation is that the 1D approach is oversimplified. Another possibility is irreversible protein binding in the detection window. Such binding is not described by the theoretical model and can cause a nonzero signal for large times in Figures 3 and 4.

We used the simplest model with reversible protein adsorption only. It can be considered as the first approximation in describing the real process of protein adsorption. To take into account irreversible protein adsorption one should introduce an additional rate constant of irreversible protein transformation[14] into the model. Such modified model could result in a better fitting in Figures 3 and 4 because we would have more fitting parameters. Nevertheless, fitting in the peak areas in these figures suggests that our simplest model of reversible protein binding at the capillary surface is quiet adequately describes the process of protein adsorption in the plug.

As a result, the following values were found: k_{ad} = (6.60 ± 1.78) mM^{-1} s^{-1}, k_{de} = (1.74 ± 0.28) × 10^{-2} s^{-1}, D = (6.11 ± 2.16) × 10^{-7} cm^{2}s^{-1}. Values of mean and standard deviations for k_{ad} and k_{de} were found using distances of both 10 and 40 cm from the injection end to the detector. To our best knowledge, there is no published data for k_{ad} and k_{de} of conalbumin on any kind of material. However, the diffusion coefficient of conalbumin from hen egg white was studied extensively resulting in the follows values of D: 5.66 × 10^{-7} and 8.4 × 10^{-7} (in two experiments),[43] 7.1 × 10^{-7} and 6.0 × 10^{-7},[44] 4.69 × 10^{-7},[45] 3.11 × 10^{-7}, and 3.21 × 10^{-7} cm^2 s^{-1}.[46] Averaging all this values gives (5.6 ± 2.1) × 10^{-7} cm^2 s^{-1}. The corresponding median value of the diffusion coefficient is 5.66 × 10^{-7} cm^2 s^{-1}. Estimation based on the empirical dependence of the diffusion coefficient on the protein molecular weight M_w[47] gives a value of 5.74 × 10^{-7} cm^2 s^{-1} for conalbumin's molecular weight of M_w = 77 kDa.[45] Finally, our estimate based on the Stokes–Einstein equation (for the diffusion coefficient) and the average diameter of conalbumin molecules found from the crystallographic structure of conalbumin[41] (PDB code 1AIV) results in D = 7.4 × 10^{-7} cm^2 s^{-1}. As a reference, we can obtain a mean value and deviation by pooling together all above values, (5.9 ± 1.9) × 10^{-7} cm^2 s^{-1}. The diffusion coefficient obtained by our 1D approach, (6.11 ± 2.16) × 10^{-7} cm^2 s^{-1}, is in excellent agreement with this reference value. This agreement confirms the validity of our fitting procedure and the 1D approach in general.

Characteristic Patterns of the Plug Propagation. A temporal signal profile from the protein passing the detector at the end of the capillary depends on three characteristic times: t_{ad}, t_{de}, and t_{det}. Figure 5 shows results of numerical simulations with the 1D model.

At $t_{ad} \geq t_{det}$, the profile has characteristic peak and trail (Figure 5A). The peak reaches the detector at $t \sim t_{det}$ and mostly results from protein that did not adsorb onto the wall during propagation. The trail corresponds to protein that adsorbed and then desorbed (potentially several times). The trail is most prominent at $t_{de} \sim t_{det}$. The trail is very steep and short if $t_{de} \ll t_{det}$, and it is very low and almost undistinguishable if $t_{de} \gg t_{det}$ (Figure 5A).

DOI: 10.1021/ac503880j
Anal. Chem. 2015, 87, 1219–1225

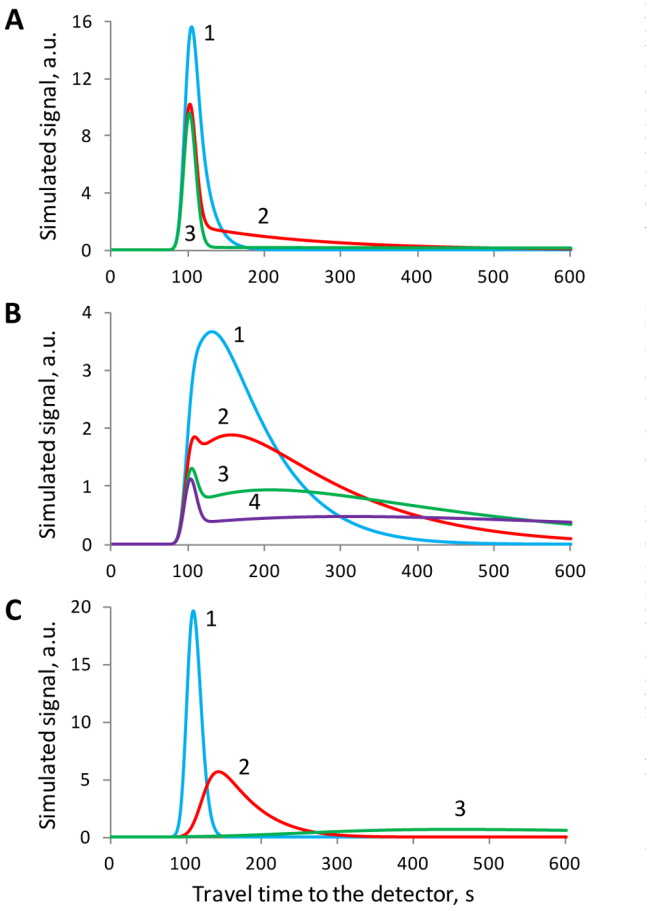

Figure 5. Simulated signals from the protein detected at the end of the capillary. The distance to the detection point is L = 10 cm. The travel time to this point is $t_{det} = L/v = 10^2$ s. Various characteristic adsorption and desorption times, t_{ad} and t_{de}, were analyzed. Panel **A** corresponds to $t_{ad} = 10^2$ s; lines 1−3 shown in blue, red, and green correspond to t_{de} = 10, 10^2, and 10^3 s, respectively. Panel **B** corresponds to t_{ad} = 25 s; lines 1−4 shown in blue, red, green, and magenta correspond to t_{de} = 25, 50, 100, and 200 s, respectively. Panel **C** corresponds to t_{ad} = 10 s; lines 1−3 shown in blue, red and green correspond to t_{de} = 1, 10, and 10^2 s, respectively.

More complex signal patterns are possible in the case of t_{ad} which is only a few times smaller than t_{det} and $t_{de} \sim t_{det}$ (Figure 5B). In this case, the not-monotonic trail with a "bump" can be observed. The bump height depends on the value of t_{de}/t_{det} (Figure 5B).

Finally, if $t_{ad} \ll t_{det}$, there is practically no protein left within the injected plug space when it reaches the detector. In this case, the peak corresponds to protein that was adsorbed and desorbed many times. As a result, the peak reaches the detector significantly later than the nonadsorbing protein would (Figure 5C with the exception of the blue line for which $t_{de} \ll t_{ad}$, and therefore, the protein quickly desorbs back to the solution). The time required for peak's reaching the detector increases with increasing t_{de}. Peaks also become lower and wider with increasing t_{de}. Again, the trail can be distinguished behind the peak at $t_{de} \sim t_{det}$ (Figure 5C). Figure 5B describes the intermediate case between Figure 5A,C. Given expressions (eq 13) for t_{ad} and t_{de} in terms of parameters $k_{ad}N_{tot}$ and k_{de}, these parameters can be qualitatively estimated by comparing experimental signal-vs-time profiles with those shown in Figure 5.

CONCLUDING REMARKS

In this work, we developed a method for studying kinetics of adsorption and desorption of protein onto a capillary wall by using averaged 1D equations of mass transfer in a capillary. This method uses the capillary itself as a flow cell and significantly reduces computation time. We compared the 1D approach to the one based on exact 2D equations and found that relative errors were less than 5%. We then applied the 1D approach to studying adsorption kinetics of conalbumin from hen egg white and determined the rate constants of adsorption and desorption (for the first time for this protein). The conalbumin diffusion coefficient was also found and proved to be in very good agreement with known experimental values and theoretical estimates. Finally, we analyzed possible characteristic signals-vs-time profiles. The developed 1D approach provides a simple and effective way of studying kinetics of reversible protein adsorption on the surface.

MATERIALS AND METHODS

Chromeo P503 fluorescent pyrylium dye was used for protein labeling as described elsewhere.[4] Experiments were performed using a P/ACE MDQ capillary electrophoresis instrument (Beckman-Coulter, Fullerton, CA) equipped with a laser-induced fluorescence (LIF) detection system. A continuous 488 nm solid-state laser line was used to excite the fluorescence of Chrome-labeled protein.

All experiments were performed using a 50 cm-long capillary (40 or 10 cm to the detection window). The internal radius of the capillary was 37.5 μm and the average flow velocity was 0.1 cm/s. The temperature was monitored during experiments and was kept at 20 °C. Repeatability of experiments was satisfactory. The coefficients of variation for determined values of k_{ad}, k_{de}, and D were 27%, 16%, and 33%, respectively, which can be explained by the approximate nature of the method used for their determination. Bare silica capillaries were pretreated by rinsing with methanol for 10 min at 20 psi. Prior to each run, the capillary was rinsed sequentially with 0.1 M HCl, 0.1 M NaOH, deionized H_2O, and 50 mM Tris acetate (pH 8.2) at 20 psi for 2 min.

Samples were introduced into the capillary by applying a 5 s (for 5.3 μM conalbumin) or 6 s (for 6.2 μM conalbumin) pressure pulse of 0.5 psi. Pressure-driven propagation analyses were carried out using the 50 mM Tris acetate (pH 8.2) run buffer. A 0.5 psi forward pressure was applied for the 40 cm propagation and a reversed pressure of the same magnitude was used for the 10 cm propagation experiments.

AUTHOR INFORMATION

Corresponding Author

*E-mail: skrylov@yorku.ca.

Notes

The authors declare no competing financial interest.

ACKNOWLEDGMENTS

The work was funded by the Natural Sciences and Engineering Research Council of Canada.

REFERENCES

(1) Schure, M. R.; Lenhoff, A. M. *Anal. Chem.* **1993**, *65*, 3024−3037.
(2) Gasš, B.; _Štědrý, M.; Kenndler, E. *Electrophoresis* **1997**, *18*, 2123−2133.
(3) Towns, J. K.; Regnier, F. E. *Anal. Chem.* **1992**, *64*, 2473−2478.

DOI: 10.1021/ac503880j
Anal. Chem. 2015, 87, 1219−1225

(4) de Jong, S.; Krylov, S. N. *Anal. Chem.* **2012**, *84*, 453−458.
(5) Chuang, I. S.; Maciel, G. E. *J. Phys. Chem. B* **1997**, *101*, 3052−3064.
(6) Fan, H.-F.; Li, F.; Zare, R. N.; Lin, K.-C. *Anal. Chem.* **2007**, *79*, 3654−3661.
(7) McCormick, R. M. *Anal. Chem.* **1988**, *60*, 2322−2328.
(8) Lauer, H. H.; McManigill, D. *Anal. Chem.* **1986**, *58*, 166−170.
(9) Towns, J. K.; Regnier, F. E. *Anal. Chem.* **1992**, *63*, 1132−1138.
(10) Regnier, F. E. *Science* **1987**, *238*, 319−323.
(11) Malmsten, M., Ed. *Biopolymers at Interfaces*, 2nd ed.; Marcel Dekker: New York, 2003; p199.
(12) Yeo, D.; Panicker, R.; Tan, L.; Yao, S. *Comb. Chem. High Throughput Screening* **2004**, *7*, 213−221.
(13) Ramsden, J. J. *Q. Rev. Biophys.* **1993**, *27*, 41−105.
(14) Krisdhasima, V.; McGuire, J.; Sproull, R. *J. Colloid Interface Sci.* **1992**, *154*, 337−350.
(15) Krisdhasima, V.; Vinaraphong, P.; McGuire, J. *J. Colloid Interface Sci.* **1993**, *161*, 325−334.
(16) Dijt, J. C.; Cohen Stuart, M. A.; Hofman, J. E.; Fleer, G. J. *Colloids Surf.* **1990**, *51*, 141−158.
(17) Dijt, J. C.; Cohen Stuart, M. A.; Fleer, G. J. *Macromolecules* **1992**, *25*, 5416−5423.
(18) Van Der Veen, M.; Cohen Stuart, M.; Norde, W. *Colloids Surf., B* **2007**, *54*, 136−142.
(19) Furst, E. M.; Pagac, E. S.; Tilton, R. D. *Ind. Eng. Chem. Res.* **1996**, *35*, 1566−1574.
(20) Ren, F. Y.; Waite, S. W.; Harris, J. M. *Anal. Chem.* **1995**, *67*, 3441−3447.
(21) Silin, V.; Weetall, H.; Vanderah, D. J. *J. Colloid Interface Sci.* **1997**, *185*, 94−103.
(22) Calonder, C.; Van Tassel, P. R. *Langmuir* **2001**, *17*, 4392−4395.
(23) Thompson, N. L.; Burghardt, T. P.; Axelrod, D. *Biophys. J.* **1981**, *33*, 435−454.
(24) Hansen, R. L.; Harris, J. M. *Anal. Chem.* **1998**, *70*, 4247−4256.
(25) Kwok, K. C.; Yeung, K. M.; Cheung, N. H. *Langmuir* **2007**, *23*, 1948−1952.
(26) Woods, D. A.; Petkov, J.; Bain, C. D. *J. Phys. Chem. B* **2011**, *115*, 7353−7363.
(27) Kolev, S. D. *Anal. Chim. Acta* **1995**, *308*, 36−66.
(28) Verzola, B.; Gelfi, C.; Righetti, G. *J. Chromatogr., A* **2000**, *868*, 85−99.
(29) Verzola, B.; Gelfi, C.; Righetti, G. *J. Chromatogr., A* **2000**, *874*, 293−303.
(30) Castellettii, L.; Verzola, B.; Gelfi, C.; Stoyanov, A.; Righetti, G. *J. Chromatogr. A* **2000**, *894*, 281−289.
(31) Tran, N. T.; Taverna, M.; Miccoli, L.; Angulo, J. F. *Electrophoresis* **2005**, *26*, 3105−3112.
(32) Levich, V. G. *Physicochemical Hydrodynamics*; Prentice-Hall: Englewood Cliffs, NJ, 1962; p 700.
(33) Gervais, T.; Jensen, K. F. *Chem. Eng. Sci.* **2006**, *61*, 1102−1121.
(34) Taylor, G. *Proc. R. Soc. A* **1954**, *A225*, 473−477.
(35) Aris, R. *Proc. R. Soc. A* **1956**, *A235*, 67−77.
(36) Frankel, I.; Brenner, H. *J. Fluid Mech.* **1989**, *204*, 97−119.
(37) Okhonin, V.; Evenhuis, C. J.; Krylov, S. N. *Anal. Chem.* **2010**, *82*, 1183−1185.
(38) Chartier, A.; Georges, J.; Mermet, J. *Chem. Phys. Lett.* **1990**, *171*, 347−352.
(39) Parker, C.; Rees, W. *Analyst* **1960**, *85*, 587−600.
(40) Kanoatov, M.; Retif, C.; Cherney, L. T.; Krylov, S. N. *Anal. Chem.* **2012**, *84*, 149−154.
(41) Kurokawa, H.; Dewan, J. C.; Mikami, B.; Sacchettini, J. C.; Hirose, M. *J. Biol. Chem.* **1999**, *274*, 28445−28452.
(42) Ong, S. W.; Zhao, X. L.; Eisenthal, K. B. *Chem. Phys. Lett.* **1992**, *191*, 327−335.
(43) Bain, J. A.; Deutsch, H. F. *J. Biol. Chem.* **1948**, *172*, 547−555.
(44) Marshall, M. E.; Deutsch, H. F. *J. Biol. Chem.* **1951**, *189*, 1−9.
(45) Rabbani, G.; Ahmad, E.; Zaidi, N.; Khan, R. H. *Cell. Biochem. Biophys.* **2011**, *61*, 551−560.
(46) Fuller, R. A.; Briggs, D. R. *Org. Biol. Chem.* **1956**, *78*, 5253−5257.
(47) Young, M. E.; Carroad, P. A.; Bell, R. L. *Biotechnol. Bioeng.* **1980**, *22*, 947−955.

DOI: 10.1021/ac503880j
Anal. Chem. 2015, 87, 1219−1225